CHAPTER 2
PHYSICS OF RADIO RECOMBINATION LINES

Physical processes occuring in gaseous nebulae in the interstellar medium are quite well understood and have now become text book material. Excellent discussions of the relevant physics and its application to the understanding of the properties of nebulae and their environment can be found for example in Osterbrock (1974), Chaisson (1976) and Spitzer (1978). The knowledge that has been gained so far is now routinely used as a tool for interpreting the observations in terms of physical properties like temperature, density, kinematics and composition of the object under study. Attempts have been, and still are being, made to put together several such pieces of information to understand the overall structure and constituents of the interstellar medium

In this chapter we present a description of the physical processes occuring in ionized regions in the galaxy known as HII regions and discuss the nature of the radiation emitted by them The processes described here will be later used for interpretation of the recombination lines observed in the present study.

2.1 PHYSICAL PROCESSES IN HII REGIONS:

HII regions are gaseous clouds in interstellar space which are more or less completely ionized by the ultraviolet radiation from one or more hot stars having surface temperatures in excess of 30,000K. Most of the observed radio recombination lines arise from such regions. By far the most abundant element in HII regions, as in practically all astronomical objects is hydrogen. It constitutes more than 90% of the matter in HII regions. The

next most abundant element is helium (~9%). Heavier elements like C, N, O, Ne, S, Ar etc are also present, in HII regions, in small quantities. Their abundance relative to hydrogen ranges from 10^{-4} to 10^{-6} by number, similar to the cosmic abundance. As will be discussed later, the heavy elements although present in very small quantities (in fact are called trace elements), they play an important role in regulating the temperature of HII regions.

The exciting star or stars of an HII region are of O- or early B- type. These stars can emit ultraviolet photons with energies greater than 13.6eV, the ionization potential of hydrogen, and these in turn ionize the gas cloud surrounding the stars. Only a finite flux of UV photons can be produced by the stars and thus they can only ionize a finite volume of the gas. Therefore if the star is in a sufficiently large cloud then the ionization can occur only up to a certain distance, outside of which the gas will be neutral. Such regions are known as 'ionization or radiation bounded' HII regions. There is usually a sharp transition between the ionized and the neutral regions; the thickness of the transition zone being one mean free path of the ionizing photons. The boundary of ionization will be rather symmetric about the exciting star and the ionized region is also known as the 'Stromgren sphere'. If there is a lack of neutral material capable of being ionized by the UV radiation then a 'density-bounded' HII region is created. Such regions will have irregular shapes given by the boundary of the gas cloud sorrounding the star. Depending on the temperature of the exciting star, helium and the heavy elements are singly or doubly ionized. As the ionization potential of the elements are different, it is possible to have different Stromgren spheres for different elements and their ionization levels within a given HII region.

Since hydrogen is the most abundant element, the energy input from the exciting star to the HII region comes from photo-ionization of hydrogen. UV photons with energies greater than 13.6eV ionize the hydrogen and the excess energy above the

ionization potential goes into the kinetic energy of the liberated electron. In a steady state the number of ionizations is balanced by a corresponding number of recombinations and an ionization equilibrium is established. Large departures from ionization equilibrium are unlikely since the typical recombination lifetime ($\sim 10^5 N_e^{-1}$ years, where N_e is the electron density) is short compared to the typical nebular lifetimes ($10^6 - 10^7$ years) even for low density regions ($N \sim 10 cm^{-3}$). Any recombination to a level with $n > 1$ is followed by rapid downward transitions at a rate given by $A \sim 10^4 - 10^8$ sec^{-1}. These radiative life times of the excited levels are exceedingly short compared to the photo-ionization life time ($\sim 10^8$ sec). Therefore the ionization of hydrogen occurs almost always from its ground state.

The photo-electrons liberated during the ionization carry the excess energy of the ionizing photons as their kinetic energy. The free electrons immediately establish a Maxwellian velocity distribution through collisions among themselves and with the ions. The cross-section for elastic collisions among electrons exeed by a large factor all other nebular corss-sections including recombination. Such collissions are almost perfectly elastic and thus the translational kinetic energy of the electrons is exchanged back and forth many times and a Maxwellian distribution of velocity among the particles is established.

In ionization equilibrium the number of ionizations is balanced by an equal number of recombinations. The difference in the energy of an electron when it was created during photo-ionization and its energy when it undergoes recombination goes into heating of the nebular gas. This is the main source of heating for the ionized region. In thermal equilibrium this heating is balanced by cooling mechanisms in which the electron loses energy through inelastic collisions with protons and particularly the heavy ions present in the nebula. The main source of cooling is the electron collisional excitation of the low lying bound levels of reasonably abundant elements such as

oxygen, nitrogen and sulphur, followed by spontaneous emission of photons which escape from the nebula. Electrons also lose some amount of energy during their other encounters with ions which result in free-free emission i.e. thermal bremsstrahlung. The temperature of the nebular gas is determined by the balance between heating by photo-ionization and cooling largely by collisional excitation of the bound levels of trace elements followed by emission of photons. The resulting temperatures are generally in the range 6000K-10000K. The factors which determine the temperature of a nebula are the abundance of' trace elements like O, N, Ne, S etc, the electron density N_e and to a lesser extent the effective temperature of the exciting star or stars. If the electron density N_e is increased, the temperature of the nebula will increase since the excited levels of the trace elements become depopulated by collisional de-excitation and not by radiative transitions which serve to cool the nebula. On the other hand an increase in the abundance of trace elements will decrease the nebular temperature as the above cooling process becomes more effective. However a high effective temperature of the exciting stars usually results in a higher ionization of the trace elements and not in a higher nebular temperature.

The Maxwellian velocity distribution of the electrons and ions in the nebula are charecterized by the nebular temperature T_e which is generally in the range of 6000K-10000K. Usually a single temperature is applicable to the velocity distribution of all the different species of particles in the gas. As a result heavier particles will have smaller velocities.

2.2 OPTICAL RADIATION FROM HII REGIONS:

Continuum optical radiation from HII regions arises mainly from two processes. One is the free-bound transition in which a free electron with a certain energy recombines to a bound atomic level. The second is the two-photon emission mechanism in which a recombined electron ending up in the $2\,^2S_{1/2}$ bound level makes a further transtion to the $1\,^2S_{1/2}$ ground level through emission of two photons. A single photon emission between these two states

is forbidden by selection rules. The individual energies of the two photons are unrestricted provided that together thoy conserve the 10. 2eV separation between the two levels.

A variety of optical spectral lines are emitted from an HII region as recombination lines and lines due to radiative transitions from collisionally excited states of the heavy ions e. g. O, N, Ne, S etc. Recombination lines occuring in the optical regime are the visible Balmer series of hydrogen and helium The population of the excited levels for these transitions is through recombination and downward cascade. The beautiful photographs of HII regions which occupy the fronticepiece of many text books are taken in such recombination lines like H_α and Hp .

The most interesting optical spectral lines are the forbidden lines emitted due to transition from excited metastable levels of [OII], [OIII], CNIII, [SII] etc (in the case of forbidden lines the chemical symbol is usually bracketed). Transitions from some of the excited levels of these ions are forbidden by selection rules for electric dipole radiation, for which the life time is of the order of 10-*seconds. However weaker electric quadrupole and magnetic dipole radiation is allowed from these leve'ls with lifetimes of the order of 1 and 10^4 seconds respectively. Even with such long life times these transitions do occur in the tenuous HII regions and the resulting lines carry important information about the nebular properties.

The long life times of the metastable excited levels against spontaneous decay make it nearly impossible to observe the forbidden lines in the laboratory. Even in the best laboratory vacuum where densities are $\sim 10^7$-10^8 cm^{-3}, collisional de-excitation ensures depopulation of the excited metastable levels before they have a chance to radiate through electric quadrupole or magnetic dipole radiation. However in HII regions, where densities are in the range of 10-10^4 cm^{-3}, the time scale for collisional de-excitation is comparable to, or even longer than, that for radiative process, permitting these forbidden lines to be observed. It is the emission of these forbidden

lines from the trace elements that is critically important as a cooling mechanism in regulating the temperature of HII regions. Such lines are also emitted in the ultraviolet and infrared region.

Fromthe measured intensities and width of the optical spectral radiation, many important properties of the HII regions like temperature, density and composition can be derived. However such studies are restricted to relatively nearby HII regions. The optical radiation fromdistant HII regions in the galaxy is generally obscured by the dust present along the line of sight. Such a restriction is however not applicable to radio radiation from these objects which also carries considerable information about the nebular properties.

2.3 RADIO CONTINUUM EMISSION:

Radio continuum radiation from an ionized gas arises from thermal bremsstrahlung, also called free-free radiation, during encounters of the free electrons in the gas with the positive ions. A simplified picture of this process is illustrated in figure 2.1. An electron of initial kinetic energy $\frac{1}{2}mv_1^2$ on coulumb interaction with a charge Ze gets deflected and radiates and goes out with a reduced final energy $\frac{1}{2}mv_2^2$. The difference between the initial and final energies is emitted as a photon which can escape from the nebula. A summation of energies lost by the electrons in several such encounters with different impact parameters b and different initial and final energies accounts for the continuum radiation from the nebula, most of which appears at radio frequencies. The radio continuum radiation, although it contributes very little to the energetics of an HII region, provides a very powerful tool for studying such objects at large distances in the galaxy, since at these frequencies interstellar extinction is practically absent.

2.3.1 Radiation Transfer

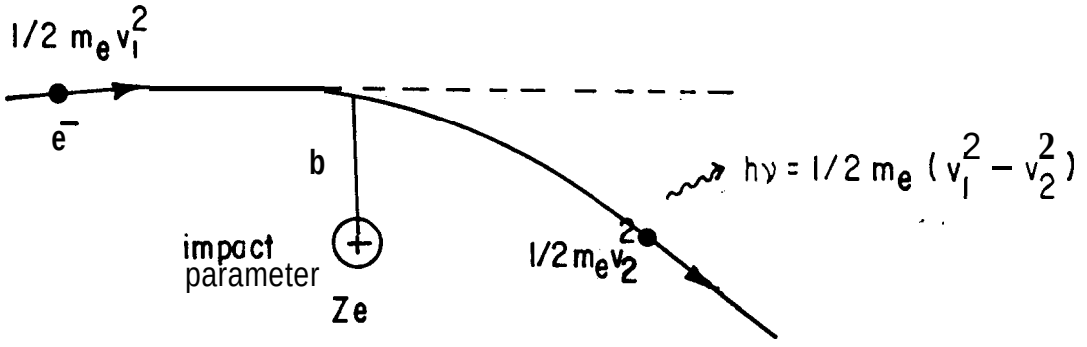

FIG. 2.1. An electron–ion encounter.

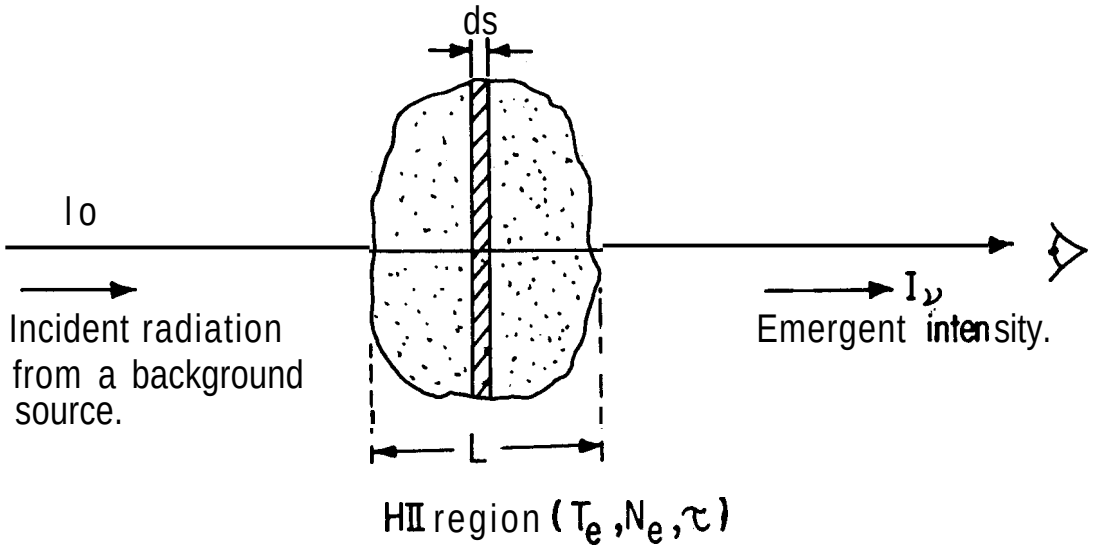

FIG. 2.2. Radiation transfer through a HII region.

The change in the specific intensity I_ν (energy/unit solid angel/unit time/unit frequency interval) in passing through a region of thickness ds (see figure 2.2) can be written as

$$dI_\nu = -k_\nu\, ds\, I_\nu + j_\nu\, ds \qquad (2.1)$$

where k_ν and j_ν are the absorption and emission coefficients at frequency ν. Introducing the differential optical depth $d\tau_\nu$ defined by $d\tau_\nu = k_\nu ds$ we get

$$\frac{dI_\nu}{d\tau_\nu} = -I_\nu + \frac{j_\nu}{k_\nu} \qquad (2.2)$$

In an HII region, the velocities of electrons, ions and atoms are determined purely by collisions, and they have a Maxwellian distribution characterized by a temperature T; and local thermodynamic equilibrium prevails. The emission and absorption of the continuum intensity I is balanced separtely at each frequency and' according to Kirchoff's law

$$\frac{j_\nu}{k_\nu} = B_\nu(T) \qquad (2.3)$$

where $B_\nu(T)$ is the Planck function given by

$$B_\nu(T) = \frac{2h\nu^3}{c^2}\left(\exp\frac{h\nu}{kT} - 1\right)^{-1} \qquad (2.4)$$

which at radio frequencies, where $h\nu/kT \ll 1$, can be written as

$$B_\nu(T) = \frac{2k\nu^2}{c^2}\cdot T \qquad (2.5)$$

which is the familiar Rayleigh-Jeans law. The transfer equation can now be written as

$$\frac{dI_\nu}{d\tau_\nu} = -I_\nu + B_\nu(T)$$

which for incident radiation $I_{o\nu}$ has the solution

$$I_\nu = I_{o\nu}\, e^{-\tau_\nu} + B_\nu(T)\,(1 - e^{-\tau_\nu}) \qquad (2.6)$$

It is conventional in radio astronomy to measure the intensity I_ν in terms of the brightness temperature $T_{b\nu}$ usually defined as the temperature at which $B_\nu(T_{b\nu})$ equals the observed intensity. In other words $T_{b\nu} = c^2 I_\nu / 2\nu^2 k$. Equation (2.6) expressed in brightness temperature becomes

$$T_{b\nu} = T_{b\nu_0} e^{-\tau_\nu} + T(1 - e^{-\tau_\nu}) \qquad (2.7)$$

Equation (2.7) is a fundamental equation in radio astronomy. It describes the characteristics of the radiation observed with a telescope (the quantity $T_{b\nu}$) in terms of the properties of the radiating region characterized by T and τ_ν. With a knowledge of τ_ν the continuum optical depth, it is possible to describe the characteristics of the continuum radiation at different frequencies.

2.3.2 The Continuum Optical Depth

We shall denote the quantities corresponding to the continuum radiation from the HII region with a subscript C. Thus the continuum optical depth, the emission and absorption coefficients are denoted by τ_c , j_c and k_c respectively. From equation (2.3) and (2.5) we can write

$$\frac{j_c}{k_c} = B(T_e) = \frac{2k\nu^2}{c^2} \cdot T_e \qquad (2.8)$$

where T_e is the temperature of the HII region usually called the electron temperature as it characterizes the Maxwellian velocity distribution of the electrons. The absorption coefficient k_c is therefore given by

$$k_c = \frac{1}{2} \cdot j_c \cdot \frac{c^2}{\nu^2} (kT_e)^{-1} \qquad (2.9)$$

If L is the total pathlength through the HII region then the continuum optical depth is given by

$$\tau_c = \int_0^L k_c \, ds \qquad (2.10)$$

From equations (2.9) and (2.10) an evaluation of the continuum emission coefficient j_c leads to the optical depth

An expression for J_c has been derived by Oster (1961). The calculation is made by first considering a single electron-ion encounter such as in figure 2.1 with a specified velocity and an impact parameter. The summation over an ensemble of encounters is made by integrating first over a suitable range of impact parameter b and then over a Maxwellian velocity distribution at temperature T_e. For a constant temperature nebula, the expression for the continuum optical depth is given by

$$\tau_c = \frac{3.014 \times 10^{-2}}{\nu^2 T_e^{3/2}} \cdot \ln\left(4.955 \times 10^{-2} \cdot \frac{T_e^{3/2}}{\nu}\right) \cdot E_c \qquad (2.11)$$

The numerical constant is a function of fundamental constants. N_e is the number density of electrons in cm^{-3} and N_i is that of the ions. ν is the frequency in GHz and the temperature T_e is in °K. E_c is known as the emission measure of the nebula. It is defined by

$$E_c = \int_0^L N_e N_i \, ds \qquad pc\ cm^{-6} \qquad (2.12)$$

An approximate expression corresponding to equation (2.11) was given by Altenhoff et al (1960) as

$$\tau_c = 8.235 \times 10^{-2} \cdot a(\nu, T_e)\, \nu^{-2.1}\, T_e^{-1.35}\, E_c \qquad (2.13)$$

where $a(\nu, T_e)$ is a slowly varying function of frequency and temperature. For frequencies of interest in the radio region $a(\nu, T_e) = 1$ is correct to within 5%.

2.3.3 The Continuum Spectrum

Using equation (2.7) for the brightness temperature and equation (2.13) for the continuum optical depth we can now describe the continuum radiation from a HII region as a function of frequency. Taking the case of an isolated HII region (no

background source) we have for the observed brightness temperature

$$T_{b\nu} = T_e \left(1 - e^{-\tau_{c\nu}}\right) \qquad (2.14)$$

where $\tau_{c\nu}$ is the continuum optical depth at a frequency ν and T_e is the' electron temperature. Two cases can be considered; the optically thin case when $\tau_{c\nu} << 1$ and the optically thick case when $\tau_{c\nu} >> 1$. We can write

$$T_{b\nu} = \begin{cases} T_e\, \tau_{c\nu} & \text{if } \tau_{c\nu} << 1 \\ T_e & \text{if } \tau_{c\nu} >> 1 \end{cases} \qquad (2.15)$$

A more meaningful quantity is the total intensity of the radiation integrated over the extent of the nebula (solid angle Ω_s) known as the flux density. It is given by

$$S_\nu = \int_{\Omega_s} I_\nu \, d\Omega = \frac{2k\nu^2}{c^2} \int_{\Omega_s} T_{b\nu} \, d\Omega \qquad (2.16)$$

If the brightness temperature is constant over the face of the nebula, then

$$S_\nu = \frac{2k\nu^2}{c^2} \cdot T_{b\nu} \cdot \Omega_s \qquad (2.17)$$

The unit of flux density is the Jansky (1 Jansky = 10^{-26} wm^{-2}Hz^{-1}). From equation (2.13), (2.15) and (2.17) we have for the flux density from an HII region in the optically thick and optically thin cases

$$S_\nu = \text{Const.}\ \frac{2k}{c^2}\, T_e^{-0.35}\, \nu^{-0.1}\, E_c \cdot \Omega_s \quad \text{for } \tau_c << 1 \qquad (2.18)$$

$$S_\nu = \frac{2k}{c^2} \cdot T_e \cdot \nu^2 \Omega_s \quad \text{for } \tau_c >> 1$$

These equations define the continuum spectrum of the HII region. At low frequencies where the HII region is optically thick, the flux is that of a black body at temperature T_e and goes as ν^2. In the optically thin region the spectrum is nearly flat with a weak dependance on frequency ($\alpha \nu^{-0.1}$). The continuum spectrum of

an HII region is illustrated in figure 2.3.

2.3.4 Properties of HII Regions from Continuum Observations

As the radio radiation is not subject to interstellar extinction, the continuum radio map of an HII region completely delineates the distribution of the nebular gas. A measurement of the continuum spectrum, such as in figure 2.3, using multifrequency radio maps, can be used to derive the electron temperature and emission measure of the HII region. According to equation (2.18) the spectrum is specified by T_e and E_c. These quantities can be varied to fit the observed spectrum The spectrum also gives the turnover frequency ν_t at which the optical depth becomes unity. ν_t in turn is related to the density temperature and size of the HII region. From equation (2.131 using $\tau_c = 1$ we get an expression for ν_t as

$$\nu_t = 0.3\, a^{1/2}(\nu, T_e)\, T_e^{-0.65}\, E_c^{1/2}$$

At sufficiently low frequencies ($\tau_c >> 1$), the observed brightness temperature is equal to the electron temperature of the HII region (eqn 2.15). If sufficient resolving power is available at low frequencies, then T_e can be directly measured.

Using a model for the distribution of gas in the HII region, and with a knowledge of its distance it is possible to derive the density, emission measure and excitation parameter of the HII region from the measured flux density and angular extent of the nebula. The excitation parameter u is defined as $u = RN_e^{2/3}$ pc cm^{-2} where R is the radius of the nebula. u is a measure of the number of Lyman continuum photons ($N(Ly_c)$) from the exciting stars. In the optically thin region the continuum radiation emitted is proportional to the absorption rate of the Lyman continuum photons ($h\nu > 13.6$eV). Therefore, from the measured flux it is possible to directly derive the quantity $N(Ly_c)$, which in turn can be used to specify the nature and number of exciting stars. From the measured size and derived density, the mass of the nebula can be estimated.

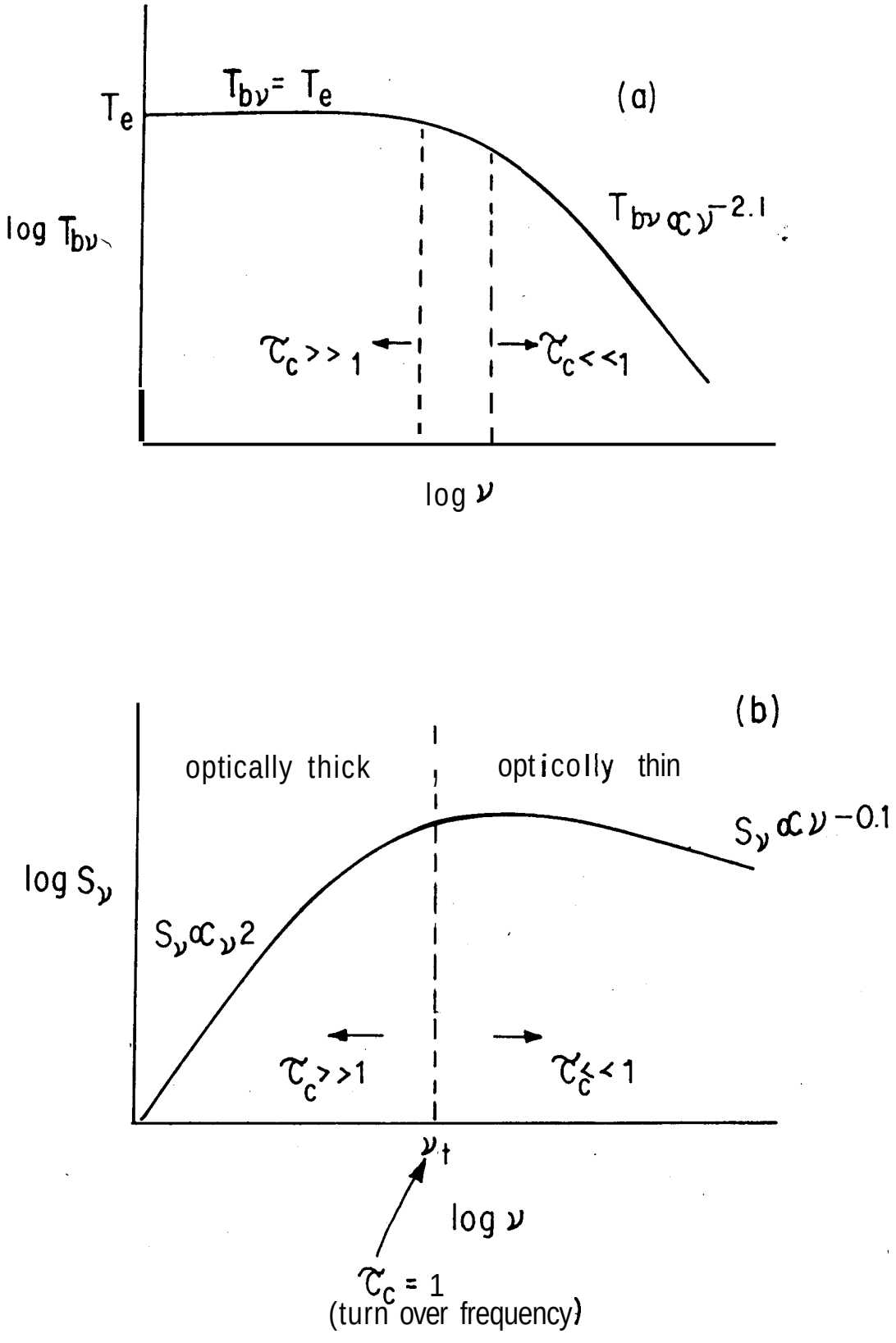

FIG. 2.3. CONTINUUM SPECTRUM OF A H II REGION
(a) In brightness temperature (b) In flux density

Many studies of such macroscopic properties of galactic HII regions have been carried out using continuum observations at different frequencies (cf. Goss and Shaver 1970, Shaver and Goss 1970a, b). From such studies it is now known that galactic HII regions have densities $N_e \sim 10\text{-}10^4 cm^{-3}$, temperature $T_e \sim 4000\text{-}9000K$, excitation parameter $u \sim 50\text{-}200$ pc cm^{-2} and sizes ranging from a few parsecs to about 30 parsecs. The total mass of the gas in an HII region varies from a few solar masses to about $10^4 M_\odot$.

2.4 RADIO RECOMBINATION ~~LINES:~~

As described earlier, in ionization equilibrium the number of photo-ionizations in the nebula is balanced by an equal number of recombinations. On recombination some of the electrons are likely to end up in very highly excited levels with principal quantum numbers $n > 500$. These electrons will eventually reach the ground state by making a series of downward transitions. The probability of making transitions with changes in principal quantum number $\Delta n = 1$ is the highest. Other transitions with $\Delta n > 1$ will also occur but with lower probability. Each such transition will result in the emission of a photon with energy corresponding to the difference in energy between the upper and lower level. When the transitions take place from principal quantum number $n > 40$, the emitted photons fall in the radio frequency range and are known as 'radio recombination lines'. Such lines have been detected from interstellar ionized regions over a wide range of frequencies from 86GHz to 26MHz, corresponding to transitions from n=42 and n=631 respectively. It. is interesting to note that the radius of the electron orbits with principal quantum number of ~ 100 is $\sim 1 \mu m$.

Radio recombination lines are denoted as $Xn\alpha$, $Xn\beta$ etc where X is the chemical symbol of the emitter and n is the principal quantum number of the lower level. Transitions with $\Delta n=1$, $\Delta n=2$ etc are denoted by α, β etc. For example $H272\alpha$ and $C272\alpha$ represent recombination lines of hydrogen and carbon respectively corresponding to transitions from n=273 to n=272.

2.4.1 Line Frequencies

The frequency of a recombination line due to a transition between an upper level and a lower level with principal quantum numbers m and n respectively is given by the Rydberg formula

$$\nu_{mn} = R_X c Z^2 \left(\frac{1}{m^2} - \frac{1}{n^2} \right) \qquad (2.19)$$

where R_X is the appropriate Rydberg constant given by

$$R_X = R_\infty \left(1 + \frac{m_e}{M_X} \right)^{-1}$$

m_e is the mass of the electron and M_X is the mass of the atomic species X. This formula can also be used for helium and heavier atoms in the radio range since for an electron in an orbit with $n > 40$ the shielding of the nucleus by the inner electrons ensures validity of the hydrogenic approximation.

The effect of fine structure splitting (the l levels) is negligible in the radio frequency range. The fine structure splitting causes a displacement in the frequency calculated according to equation (2.19) by no more than $5 \times 10^{-7} \nu$. Even for heavier emitters, the correction to equation (2.19) due to the quantum defect $\delta_{n,l}$ is also negligible, since all of the line emission in the radio frequency range comes from states with large values of the orbital angular momentum l.

A convenient approximation for calculating the recombination line frequency is

$$\nu_n = 2 R_X c Z^2 \frac{\Delta n}{n^3} \left(1 - \frac{3}{2} \frac{\Delta n}{n} \right) \qquad (2.20)$$

2.4.2 Observable Quantities

As stated earlier, in radio astronomy it is conventional to express the intensity of radiation at a frequency ν in units of

brightness temperature using the Rayleigh-Jeans approximation to the Planck black body radiation formula. The brightness temperature is given by

$$T_{b\nu} = \frac{c^2}{2k\nu^2} \cdot I_\nu$$

It should be noted that in general the brightness temperature may not be the same as the kinetic temperature of the source emitting the radiation. It is the equivalent temperature of a black body which emits the same amount of radiation as the given source at a given frequency. The brightness temperature of a source can therefore vary as a function of frequency depending on the spectrum of the emitted radiation (see for example figure 2.3a).

The observable parameters of a recombination line from an HII region are illustrated in figure 2.4 in terms of brightness temperature. A spectral line of peak brightness temperature T_{BL} appears superposed over an underlying intensity represented by T_{Bsys}. In general T_{Bsys} is made of three parts. T_{BC} the continuum brightness temperature of the HII region, T_{BN} the nonthermal background radiation present in that direction (there may also be a thermal contribution to the background) and the noise present in the observing system known as the receiver temperature T_R. The relative values of T_{BC}, T_{BN} and T_R depends on the frequency and direction of observation and the parameters of the telescope system like its angular resolution, beam efficiency, receiver temperature etc.

The centre frequency of the spectral line is ν, which may be shifted with respect to its expected frequency ν_0 (given by equation 2.19). This shift is due to the doppler effect, if the source has a motion along the line of sight. The frequency shift is given by the non-relativistic doppler formula

$$(\nu - \nu_0) = -\frac{\nu_0}{c} V \qquad (2.21)$$

where V is the velocity of the source along the line of sight. By convention v is considered positive when the source is

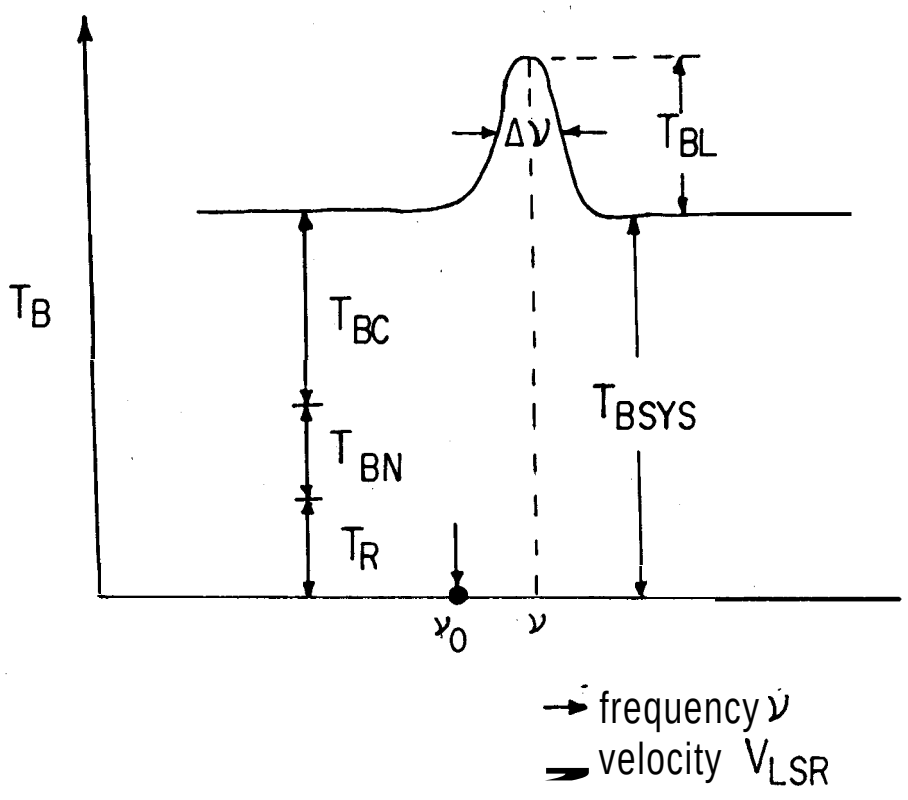

FIG. 2.4. OBSERVABLE QUANTITIES OF A RECOMBINATION LINE.

moving away from the observer. In most radio spectral line work the velocity of a source is measured with respect to local standard of rest (LSR).

The width of the spectral line (full width at half intensity) is Δv. The shape of the spectral line profile depends on the emission process and velocity fields within the emitter. For pure doppler broadening the line shape is a gaussian. The shape of recombination lines is discussed later.

It is conventional in radio spectral line work to use the velocity units defined by equation (2.21) to represent the line centre and width. The advantage is that these units are independent of frequency and directly represent one of the source properties.

A radio telescope does not directly measure the intensity of radiation in brightness temperature units as defined in fig 2.4, but it measures what is known as the antenna temperature. The relationship between the measured antenna temperature T_{AL} and the brightness temperature T_{BL} is given by

$$T_{AL} = \eta_B \cdot \frac{1}{\Omega_B} \int_{4\pi} T_{BL}(\Omega)\, f(\Omega)\, d\Omega \qquad (2.22)$$

where η_B is the main beam efficiency defined by

$$\eta_B = \int_{\text{main beam}} f(\Omega)\, d\Omega \Big/ \int_{4\pi} f(\Omega)\, d\Omega$$

where $f(\Omega)$ is the antenna response pattern normalized to unity at the peak and Ω_B is the main beam solid angle given by the numerator of the above equation. $T_{BL}(\Omega)$ represents the distribution of the line brightness temperature over the source. It can also be written as

$$T_{BL}(\Omega) = T_{BL} \cdot \psi(\Omega) \qquad (2.23)$$

where $\psi(\Omega)$ represents the angular distribution of the line emitting source with $\psi_{max}=1$. The equivalent solid angle of the

source is given by

$$\Omega_s = \int_{4\pi} \psi(\Omega)\, d\Omega$$

and the effective source solid angle modified by the antenna beam pattern is

$$\Omega_s' = \int_{4\pi} \psi(\Omega) f(\Omega) d\Omega = \begin{cases} \Omega_s & \text{if } \Omega_s \ll \Omega_B \\ \Omega_B & \text{if } \Omega_s \gg \Omega_B \end{cases} \qquad (2.24)$$

From equations (2.22), (2.23) and (2.24) we have

$$T_{AL} = \eta_B \cdot \frac{\Omega_s'}{\Omega_B} \cdot T_{BL} \qquad (2.25)$$

Therefore the observed line antenna temperature

$$T_{AL} = \begin{cases} \eta_B T_{BL} & \text{if } \Omega_s \gg \Omega_B \\ \eta_B \frac{\Omega_s}{\Omega_B} T_{BL} & \text{if } \Omega_s \ll \Omega_B \end{cases} \qquad (2.26)$$

The factor Ω_s'/Ω_B is often known as the beam dilution. Similar equations apply for the observed continuum antenna temperature.

Generally, it is difficult to accurately determine experimentally the quantities η_B and Ω_s'. Therefore it is usually a problem to convert the measured line or continuum intensity in antenna temperature units to the universal brightness temperature units. The problem will be somewhat alleviated if one measures the line to continuum intensity ratio, which to first order is independent of system parameters. For this ratio we have

$$\frac{T_{AL}}{T_{AC}} = \frac{\Omega_{sL}'}{\Omega_{sC}'} \frac{T_{BL}}{T_{BC}} \qquad (2.27)$$

where Ω_{sL}' and Ω_{sC}' are the modified source solid angle for the line and continuum emitting regions. In recombination line work at high frequencies (> few GHz), it is usually assumed that the continuum and line radiation originate from the same projected area. This is more or less true for isolated HII regions as the non-thermal background is considerably weakened at high frequencies due to its steep spectrum We then have

$$\frac{T_{BL}}{T_{BC}} = \frac{T_{AL}}{T_{AC}} \qquad (2.28)$$

As will be shown later, this line to continuum ratio for an HII region is directly related to the electron temperature of the nebula on the assumption of homogeneity in density and temperature. Such measurements have been used in many studies to deduce the electron temperatures of HII regions.

However in many situations, particularly at low frequencies (<500MHz) and in observations in the galactic plane, the assumption that the line and continuum radiation originate from the same volume or even the same projected area is not valid. This is because of two reasons. One is that the non-thermal galactic background is most intense at low frequencies and it dominates the observed continuum radiation. Secondly, at low frequencies the beam solid angles are usually large and the beam dilution (Ω_{sc}/Ω_B) is more severe for HII regions which usually have small angular sizes than for the non-thermal background which extends over large areas. At low frequencies the assumption is unlikely to be valid even for isolated HII regions (no non-thermal background), for yet another reason. HII regions are known to have density inhomogenities. As will be shown later, low frequency recombination lines originate predominantly in low density regions which contribute very little to the continuum radiation. The dominant contribution to the contiuum radiation (which is $\propto \int N_e^2 dl$) is from higher density regions.

For these reasons the line to continuum intensity ratio at low frequencies may not have any direct physical meaning. Nevertheless it is practical to measure this ratio even at low frequencies, to remove the dependence on system parameters. Care should be taken while interpreting this ratio in terms of the physical properties of the line emitting region. Further, for the same reasons it is not advisable to compare the line to continuum intensity ratios at different frequencies as it may lead to false conclusions about the physical parameters of the source.

2.4.3 Line Radiation Transfer

We can generalize equation (2.1) to include emission and absorption for both line and continuum radiation and also the non-thermal galactic background. The change in the specfic intensity in passing through a thickness ds (see fig 2.2) is

$$dI_\nu = (-k_{L\nu} I_\nu ds + j_{L\nu} ds) + (j_{C\nu} ds - k_{C\nu} I_\nu ds) + j_{N\nu} ds \qquad (2.29)$$

where the subscrips L, C and N stand for line, thermal continuum and the non-thermal distributed background respectively. The non-thermal absorption process is not important. Introducing the differential optical depth

$$d\tau_\nu = (k_{L\nu} + k_{C\nu}) ds = k_\nu ds$$

we get

$$\frac{dI_\nu}{d\tau_\nu} = -I_\nu + \frac{j_\nu}{k_\nu} + \frac{j_{N\nu}}{k_\nu} \qquad (2.30)$$

where $j_\nu = j_{L\nu} + j_{C\nu}$ is the total thermal emission coefficient. The thermal source function S_ν is defined by

$$S_\nu = \frac{j_{L\nu} + j_{C\nu}}{k_{L\nu} + k_{C\nu}} = \frac{j_\nu}{k_\nu} \qquad (2.31)$$

If L is the extent of the line emitting region along the line of sight we have for the non-thermal intensity $I_{N\nu}$ originating in this region

$$I_{N\nu} = \langle j_{N\nu} \rangle L$$

The equation (2.30) now becomes

$$\frac{dI_\nu}{d\tau_\nu} = -I_\nu + S_\nu + \frac{I_{N\nu}}{\tau_\nu} \qquad (2.32)$$

where $\tau_\nu = (k_{L\nu} + k_{C\nu}) L = k_\nu L$ is the total optical depth. If $I_{o\nu}$ is the radiation incident on the region then the solution of the equation (2.32) is given by

$$I_\nu = I_{o\nu} e^{-\tau_\nu} + S_\nu (1 - e^{-\tau_\nu}) + \frac{I_{N\nu}}{\tau_\nu} (1 - e^{-\tau_\nu}) \qquad (2.33)$$

Equation (2.33) fully describes both the line and continuum radiation. It is necessary to specify the thermal source function S_ν to describe the nature of the radiation. In thermodynamic equilibrium the thermal source function is nothing but the universal Planck function $B_\nu(T_e)$ given in equation (2.4), which at radio frequencies (where Rayleigh-Jeans approximation applies) gives us

$$S_\nu = B_\nu(T_e) = \frac{2k\nu^2}{c^2} T_e$$

Converting the specific intensity I to brightness temperature units (using eqn 2.21) we can rewrite equation (2.33) as

$$T_{b\nu} = T_{0\nu} e^{-\tau_\nu} + T_e (1-e^{-\tau_\nu}) + \frac{T_{N\nu}}{\tau_\nu} (1-e^{-\tau_\nu}) \qquad (2.34)$$

When ν is at the line frequency, then $T_{b\nu}$ corresponds to the total line and continuum radiation. The total optical depth τ_ν is given by

$$\tau_\nu = \tau_{L\nu} + \tau_{c\nu}$$

which is the sum of the line and continuum optical depths. We will drop the subscript from here onwards and denote the quantities corresponding to line, continuum and total line plus continuum with subscripts L, C and L+C. We rewrite the equation (2.34) as

$$T_{L+C} = T_0 e^{-(\tau_L+\tau_c)} + T_e (1-e^{-(\tau_L+\tau_c)}) + \frac{T_N}{\tau_L+\tau_c} (1-e^{-(\tau_L+\tau_c)}) \qquad (2.35)$$

Outside the line frequency we only have continuum radiation and $\tau_L = 0$. Therefore

$$T_c = T_0 e^{-\tau_c} + T_e (1-e^{-\tau_c}) + \frac{T_N}{\tau_c} (1-e^{-\tau_c}) \qquad (2.36)$$

The line brightness temperature is usually measured as the excess temperature over the continuum. For an isolated HII region in the absence of any background source and non-thermal radiation (viz. $T_0 = T_N = 0$) we have for the line brightness temperature

$$T_{LB} = T_{L+C} - T_c = T_e e^{-\tau_c} (1-e^{-\tau_L}) \qquad (2.37)$$

2.4.4 LTE Line Optical Depth

To understand the nature of recombination line radiation at different frequencies using equation (2.37) it is essential to obtain expressions for the line and continuum optical depths τ_L and τ_c. The continuum optical depth τ_c has already been discussed in section 2.3.2. We now discuss the derivation of the line optical depth on the assumption of local thermodynamic equilibrium (LTE). The method followed here is similar to that of Brocklehurst and Seaton (1972). LTE is discussed in detail in section 2.5.

Quantities computed on the assumption of LTE are usually denoted with a superscript asterisk (*). The LTE optical depth through a nebula of path length L is given by

$$\tau_L^* = \int_0^L K_L^* \, ds \qquad (2.38)$$

where K_L^* is the LTE 'line absorption coefficient which is generally given by the net difference between absorption and emission, as electrons transit between an upper level m and a lower level n, due to the incident radiation. Therefore

$$K_L^* = \frac{h\nu}{4\pi} \left(N_n^* B_{nm} - N_m^* B_{mn} \right) \phi_L(\nu) \qquad (2.39)$$

B_{nm} and B_{mn} are the Einstein coefficients for the rate of absorption and stimulated emission respectively. N_n^* and N_m^* are the population of the states n and m in LTE. The degree of absorption at any frequency is modulated by the spectral profile function $\phi_L(\nu)$. Usually the line shape function is the same for both emission and absorption between any two levels of interest for radio recombination lines.

The Einstein coefficeints are related by

$$g_n B_{nm} = g_m B_{mn} \qquad (2.40)$$

where g_n and g_m are the statistical weights of the levels n and m.

In LTE the ratio of populations of levels n and m is given by the Boltzmann formula

$$\frac{N_m^*}{N_n^*} = \frac{g_m}{g_n} e^{-h\nu/kT_{ex}} \qquad (2.41)$$

where T_{ex} is known as the excitation temperature and is equal to the electron temperature (kinetic temperature) T_e if LTE prevails. Using equations (2.40) and (2.41) we can rewrite (2.39) as

$$K_L^* = \frac{h\nu}{4\pi} \phi_L(\nu) B_{nm} N_n^* \left(1 - e^{-h\nu/kT_e}\right) \qquad (2.42)$$

where the factor $(1 - \exp(-h\nu/kT_e))$ can be recognized as the correction due to the stimulated emission. The absorption rate B_{nm} is related to the Einstein spontaneous transition probability coefficient A by

$$A_{mn} = \frac{2h\nu^3}{c^2} B_{mn} = \frac{2h\nu^3}{c^2} \frac{g_n}{g_m} B_{nm} \qquad (2.43)$$

A_{mn} in turn can be written in terms of the oscillator strength f_{nm} as

$$A = \frac{8\pi^2 e^2 \nu^2}{mec^3} \frac{g_n}{g_m} f_{nm} . \qquad (2.44)$$

For $n >> \Delta n = (m-n)$ Menzel(1968) has given an expression for the oscillator strength f_{nm} as

$$f_{nm} = n K(\Delta n) \left[1 + 1.5 \frac{\Delta n}{n}\right] \qquad (2.45)$$

where $K(1) = 0.1908$, $K(2) = 0.02633$, $K(3) = 0.0810...$. In LTE the population of level n is given by the Saha equation

$$N_n^* = N_e N_i \left(\frac{h^2}{2\pi m_e kT_e}\right)^{3/2} \frac{g_n}{2P_i} e^{-h\nu_{n\infty}/kT_e} \qquad (2.46)$$

$\nu_{n\infty}$ is calculated using the Rydberg formula (2.19). N_e is the density of ions and P_i is the partition function. For hydrogen $N_i = N_{H^+}$ the number of hydrogen ions and $P_i = 1$. The statistical weight $g_n = 2n^2$. Substituting the appropriate quantities from

equations (2.43) to (2.45) into equation (2.42) and evaluating the constants we get

$$K_L^* = 1.071 \times 10^4 \, \phi(\nu) \, \frac{\Delta n}{n} \, f_{nm} \, \frac{N_e N_{H^+}}{T_e^{5/2}} \cdot \exp\left(\frac{157890}{n^2 T_e}\right) pc^{-1} \qquad (2.47)$$

Here $\phi(\nu)$ is in kHz, ν is in GHz, N_e and N_{H^+} in cm^{-3} and T_e in °K. It is assumed that $h\nu/kT_e << 1$ From equation (2.38) the LTE optical depth is given by

$$\tau_L^* = 1.071 \times 10^4 \, \phi(\nu) \, \frac{\Delta n}{n} \, f_{nm} \, T_e^{-2.5} \exp\left(\frac{157890}{n^2 T_e}\right) E_L \qquad (2.48)$$

where E_L is the line emission measure defined by

$$E_L = \int_0^L N_e N_{H^+} \, ds \quad pc \, cm^{-6} \qquad (2.49)$$

2.4.5 The Line Profile Function

The line profile function $\phi(\nu)$ essentially gives the probability distribution of atoms making transitions betwen two given levels by emitting or absorbing photons in the frequency interval $(\nu, \nu+d\nu)$. It was implicitly assumed in the above derivation of the LTE optical depth that the profile function $\phi(\nu)$ is same for both emission and absorption. This is a valid assumption when the levels are populated according to LTE. When collisional processes dominate, as shown later to be the case in the formation of radio recombination lines, weak collisions re-distribute the energy within the sublevels, 'into an LTE population on the average, before an emission or an absorption occurs. As $\phi(\nu)$ is a probability distribution it has the property

$$\int_{-\infty}^{\infty} \phi(\nu) \, d\nu = 1$$

Principally, two mechanisms contribute to the width of recombination lines; doppler broadening due to the relative motions of the atoms emitting the line, and pressure or impact broadening due to the perturbation of the energy levels of the

emitting at'oms through interaction of the emitter with its environment.

There are two components to the relative motion of line emitting atoms. One is the thermal motion of the gas due to its kinetic temperature T_e, and the other is the macroscopic turbulence in the gas. The thermal motion is described by a Maxwellian velocity distribution of the atoms and the resulting line shape is a gaussian. It is generally assumed that the macroscopic motions produce a gaussian line shape. The doppler profile function is given by

$$\phi_{LD}(\nu) = \frac{1}{\sqrt{\pi}\,\Delta\nu_D} \exp\left[-\left(\frac{\nu-\nu_0}{\Delta\nu_D}\right)^2\right] \qquad (2.50)$$

ν_0 is the frequency of the line centre. $\Delta\nu_D$ is the doppler width which is related to the full line width at half intensity $\Delta\nu_{LD}$ by

$$\Delta\nu_D = \frac{\Delta\nu_{LD}}{2\sqrt{\ln 2}} = \frac{\nu}{c}\left[\frac{2kT_e}{M_{x^+}} + \frac{2}{3}\langle v_t^2\rangle\right]^{1/2} = \frac{\nu}{c}\left[\frac{2kT_D}{M_{x^+}}\right]^{1/2} \qquad (2.51)$$

where $\langle v_t^2\rangle^{1/2}$ is the rms turbulent velocity. M_{x^+} is the mass of the emitting atom T_D is known as the effective doppler temperature.

For the low densities prevailing in HII regions, the pressure broadening was shown by Griem(1967) to be primarily due to collisions rather than to quasi-static electric fields (Stark effect). When the time between the collisions is shorter than the life time of the excited level the energy distribution of the radiative transition is altered; classically speaking, the wavetrain'is abruptly terminated due to the collision. In HII regions, electron collisions are more important than proton impacts. The line profile emitted by an assembly of atoms undergoing such collisions will be approximately a Lorentzian (Griem 1967, Peach 1972) and is given by

$$\phi_{LP} = \frac{\Delta\nu_{LP}}{2\pi} \frac{1}{(\nu-\nu_0)^2 + \left(\frac{\Delta\nu_{LP}}{2}\right)^2} \qquad (2.52)$$

where $\Delta\nu_{LP}$ is the profile width due to pressure broadening.

Brockelhurst and Leeman (1971) have computed $\Delta\nu_{LP}$ under the impact approximation and find it to be

$$\Delta\nu_{LP} = 3.74 \times 10^{-11} \frac{N_e}{T_e^{0.1}} n^{4.4} \quad kHz \qquad (2.53)$$

where n is the principal quantum number, and N_e is the electron density. From equation (2.51) and (2.53) the ratio of half power widths due to pressure and doppler broadening is

$$\frac{\Delta\nu_{LP}}{\Delta\nu_{LD}} = 7.98 \times 10^{-18} \frac{N_e}{T_e^{0.1} T_D^{0.5}} \frac{n^{7.4}}{\Delta n} \qquad (2.54)$$

The Rydberg formula has been used for the frequency ν. When both doppler and pressure broadening are present, the final line profile will be a convolution of the gaussian profile (eqn 2.50) with the Lorentzian one (eqn 2.52) which results in the so called Voigt profile. The Voigt profile can be expressed as

$$\phi_L(\nu) = \frac{1}{\Delta\nu_D \sqrt{\pi}} H(a, u) \qquad (2.55)$$

where H(a, u) is the Voigt function given by

$$H(a,u) = \frac{a}{\pi} \int_{-\infty}^{\infty} \frac{e^{-y^2}}{(u-y)^2 + a^2} dy \qquad (2.56)$$

here $a = \Delta\nu_{LP}/\Delta\nu_{LD}$, $u = (\nu - \nu_0)/\Delta\nu_D$ and $y = \nu/\Delta\nu_D$. The Voigt function has been tabulated by Harris (1948) and Posener (1959) for values of astronomical interest. Using an approximation to the Voigt function were can write the value of $\phi_L(\nu)$ at the line centre as

$$\phi_L(\nu_0) = \frac{1}{\Delta\nu_{LD}} \left[1 + 1.48 \frac{\Delta\nu_{LP}}{\Delta\nu_{LD}} \right]^{-1} \qquad (2.57)$$

The LTE optical depth at the line center corresponding to equation (2.48) can be now evaluated using (2.51), (2.54) and (2.57).

2.4.6 Intensity and Width of the Lines in LTE

For an isolated HII region with uniform temperature T_e and in the absence of any background source, the line brightness temperature is given by equation (2.37) which can be written in LTE as

$$T_{LB} = T_e \cdot e^{-\tau_c} \left(1 - e^{-\tau_L^*}\right) \qquad (2.58)$$

The LTE optical depth (eqn 2.48) τ_L^* is usually of the order of 10^{-3} for typical densities and temperatures in HII regions. Therefore the quantity $(1 - e^{-\tau_L^*})$ can be approximated by τ_L^* using the Taylor series expansion. We get

$$T_{LB} = T_e \, \tau_L^* \, e^{-\tau_c} \quad \text{for } \tau_L^* \ll 1 \qquad (2.59)$$

Using equation (2.4) the ratio of line to continuum brightness temperature is given by

$$\frac{T_{LB}}{T_{CB}} = \frac{\tau_L^* \, e^{-\tau_c}}{1 - e^{-\tau_c}} \qquad (2.60)$$

Two limiting cases when the HII region is optically thin in the continuum ($\tau_c \ll 1$), and when it is optically thick ($\tau_c \gg 1$) can be distinguished. We have

$$\frac{T_{LB}}{T_{CB}} = \begin{cases} \tau_L^* / \tau_c & \text{for } \tau_c \ll 1, \ \tau_L^* \ll 1 \\ \tau_L^* \, e^{-\tau_c} & \text{for } \tau_c \gg 1, \ \tau_L^* \ll 1 \end{cases} \qquad (2.61)$$

From the above equation it is immediately apparent that the detectability of recombination lines improves at high frequencies where $\tau_c \ll 1$ (see eqn 2.13). Below the turnover frequency ν_t where the continuum optical depth τ_c exceeds unity (ν_t is usually < 1GHz) the lines progressively merge with the continuum. This situation is illustrated in fig2.5. From equation (2.59) when the region is optically thin ($\tau_c \ll 1$)

$$T_{LB} = T_e \, \tau_L^*$$

For pure doppler broadening according to equation (2.48) and (2.51) $\tau_L^* \propto \nu^{-1}$, whence the flux in the line $S_{\nu L} = \frac{2k\nu^2}{c^2} \cdot T_{LB} \propto \nu$; Whereas the continuum flux $S_{\nu c} \propto \nu^{-0.1}$ according to equation

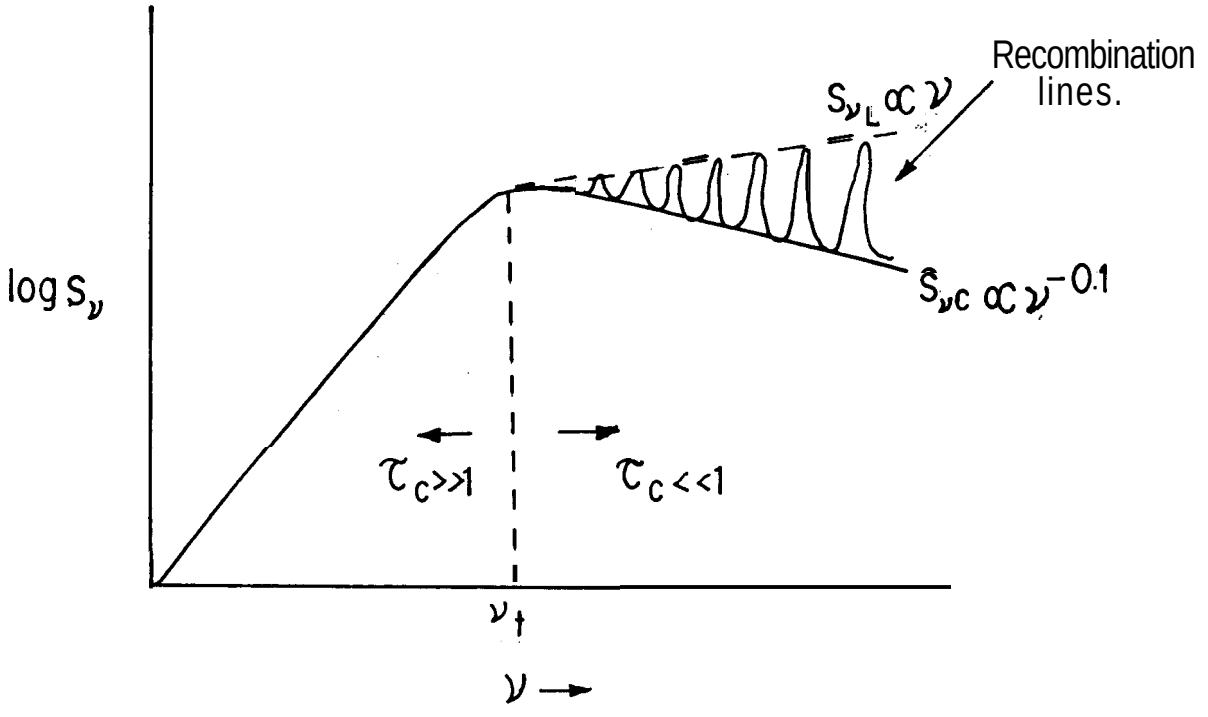

FIG. 2.5. RECOMBINATION LINE & CONTINUM FLUX FROM AN HII REGION AS A FN - OF FREQUENCY.

(2.18).

It is clear from the above discussion and fig 2.5 that recombination lines at low frequencies (< 1GHz) can only be observed fromlower density gas for which the turnover frequency ν_t is lower, and the region will still remain optically thin. When it becomes optically thick, the lines merge with the continuum

In the optically thin case, the ratio of line to continuum temperature in equation (2.16) can be explicitly written using the expressions for the continuum and line optical depths from equation (2.13) and (2.18). Assuming pure doppler broadening, the LTE optical depth at the line centre for the α lines ($\Delta n = 1$) can be written using eqns (2.48) and (2.50) as

$$\tau_L^* = \frac{1.92 \times 10^3}{\Delta\nu_{LD}\, T_e^{1.5}} E_L \qquad (2.62)$$

The exponential quantity in eqn (2.48) is ~ 1. Whence

$$\frac{T_{LB}}{T_{CB}} = \frac{\tau_L^*}{\tau_C} = 2.33 \times 10^4 \frac{\nu^{2.1}}{\Delta\nu_{LD}} T_e^{-1.15} \frac{E_L}{E_C} \qquad (2.63)$$

Here ν is in GHz and $\Delta\nu_{LD}$ is in kHz. The line emission measure $E_L = (N_e N_{H^+})L$, where L is the pathlength through the nebula and continuum emission measure $E_C = N_e N_i L = N_e(N_{H^+} + N_{He^+})L$ since hydrogen and helium account for most of the ions. Therefore

$$\frac{E_L}{E_C} = \frac{N_{H^+}}{N_{H^+} + N_{He^+}} = 1 \Big/ \left(1 + \frac{N_{He^+}}{N_{H^+}}\right) \qquad (2.64)$$

For most HII regions $N_{He^+}/N_{H^+} \sim 0.1$. Equation (2.63) directly relates the line to continuum ratio to the electron temperature T_e of the nebula. This equation has been employed in many studies of high frequency recombination lines to deduce the electron temperature of galactic HII regions. It should be remembered that this equation is based on the assumption that LTE prevails in the nebula and that there are no temperature and density inhomogeneities. Therefore care should be excercised

while applying equation (2.63) to derive the electron temperature if there are non-LTE effects and variations in temperature and density. Shaver (1980) has shown that it is possible to choose a particular frequency, depending on the emission measure of the HII region, where the above equation can be used to get accurate electron temperatures.

The width of the recombination line can be evaluated using equations (2.51) and (2.53) for doppler and pressure broadening respectively. The effective final width of the line can be approximated by

$$\Delta\nu_L^2 = \Delta\nu_{LD}^2 + \Delta\nu_{LP}^2 \qquad (2.65)$$

In reality, the contribution to the doppler broadening from pure thermal motions is no more than 50% of the observed line width. For a typical temperature of 8000K the doppler width due to thermal motions is only about 12km/s whereas the observed width of recombination lines is 25-30km/s. The rest of the width is usually attributed to macroscopic motions.

The effective width of the line calculated using equations (2.65), (2.51) and (2.53) for an HII region of temperature 8000K and different densities is shown in figure 2.6. An rms turbulence $\langle v_t^2 \rangle^{1/2}$ of 20km/s was assumed for all cases. The transition from the doppler- to the pressure- broadenlng regime can be clearly seen in figure 2.6 as a sharp minimum in the width. At lower frequencies the profile width is dominated by pressure broadening and it increases with decreasing frequency. The dot on each curve indicates the frequency at which the continuum optical depth becomes unity, and the lines begin to merge with the continuum (a path length of 20pc was assumed for all cases). It is interesting that the pressure broadening becomes dominant only below frequencies where the region is optically thick. This makes it difficult to observe pressure broadening in recombination lines. So far there is no observation which clearly indicates any pressure broadening, perhaps because of this reason.

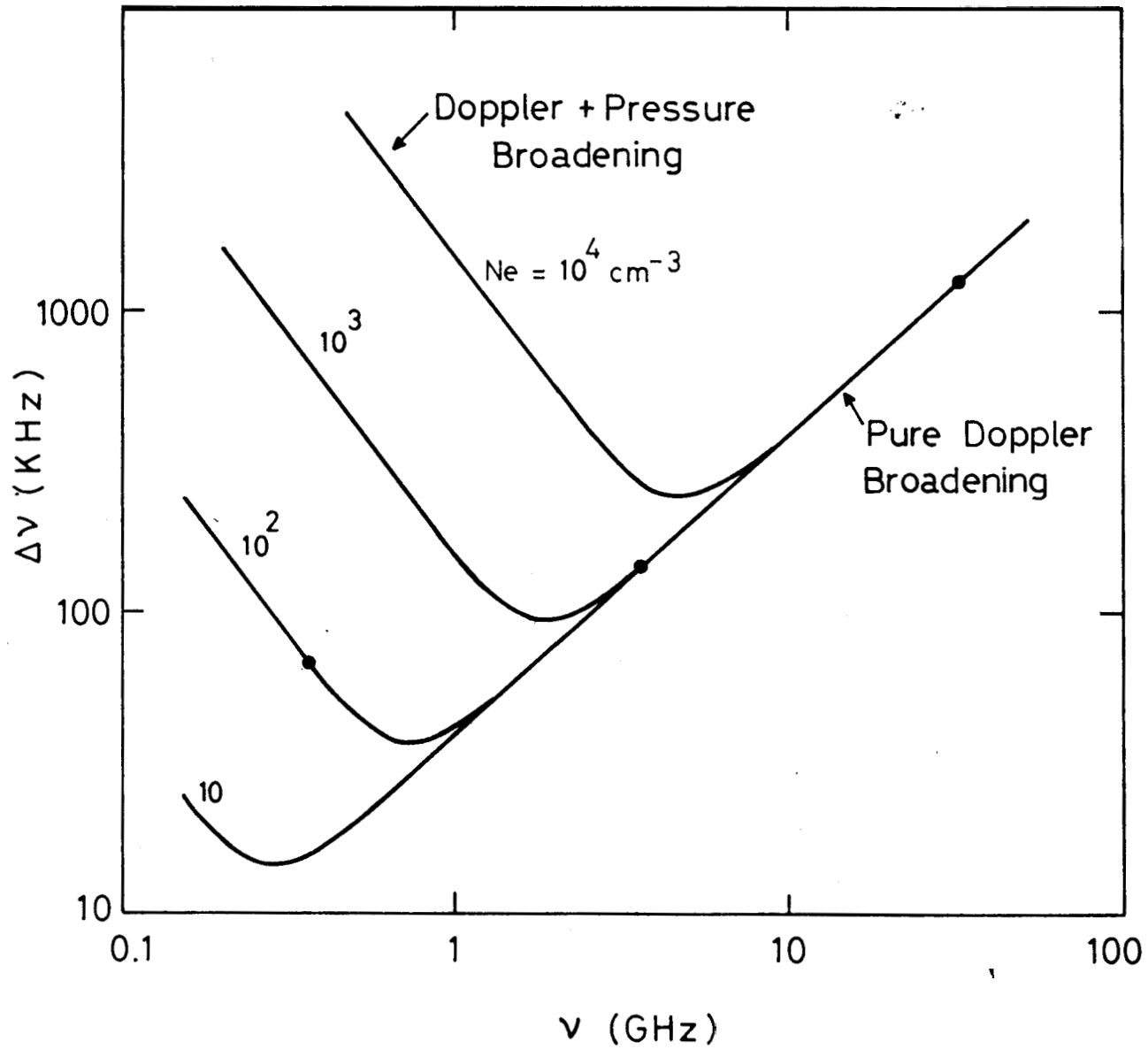

Fig. 2.6 Width of recombination lines as a function of frequency for different densities N_e, and a fixed T_e of 8000K. The dots indicate the turnover frequency ($\tau_c = 1$) assuming a pathlength of 20 pc.

An additional problem which usually makes it difficult to detect the broad Lorentzian wings in the line profile due to pressure broadening, is the instrumental baseline curvature which is inherent to any spectral line receiver. The broad wings, even if they are present, presumably get removed during the baseline fitting.

The main effect of pressure broadening is that it removes the energy in the line centre and spreads it into the broad Lorentzian wings making it difficult to detect recombination lines at lower frequencies. This is an additional reason (apart from the optical depth effect discussed before) which makes low density regions dominate in low frequency recombination line observations such as those reported in this thesis.

2.5 NON-LTE EFFECTS IN THE FORMATION OF RECOMBINATION LINES

The discussion in the previous section was based on the assumption that local thermodynamic equilibrium (LTE) prevails in the HII regions. For LTE to be true there are several conditions that must be satisfied simultaneously. For example, the velocities of the particles in the gas should follow a Maxwellian distribution; the population of the quantum states of the atoms, molecules and ions in the gas should follow the Boltzmann distribution. It will then follow that the relative population of any level of ionization of a species to that of the neutral species is given by Saha's equation. In true or complete thermodynamic equilibrium (TE), in addition to the above conditions, the spectral density of radiation should be according to Planck's law; the total energy density of radiation should be proportional to the fourth power of the temperature as per the Stefan-Boltzmann law; and detailed balancing must exist, that is every process occuring in the gas should be precisely balanced by a corresponding equal and reverse process.

In other words, in LTE the excitation temperature (T_{ex}) which characterizes the relative populations of the quantum levels in the Boltzmann law should be same as the kinetic

temperature (T_K) which characterizes the velocity of particles in the Maxwellian distribution. In TE, in additon, these should be equal to the temperature which characterizes the spectral distribution of radiation in Planck's law.

Given a Maxwellian velocity distribution of particles in a gas, the relative population of the quantumstates tends to approach a Boltzrnann distribution if the dominant process of populating the levels is collisional excitation and de-excitation, and transitions due to radiative processes are less important. Such conditions are possible if the radiative life times of the quantum levels are much longer than the rates of collision induced transitions. The gas then achieves a state of LTE. Namely the material particles will have a Maxwellian velocity distribution, the population of quantum levels a Boltzmann distribution and there will be very little coupling of matter to the radiation field. It is usual to talk of LTE for specific quantum states when their excitation temperature is equal to the kinetic temperature of the gas, even when other states do not satisfy this condition.

When the level populations do not a follow a Boltzmann distribution, then there will be departures from LTE and the situation is usually known as non-LTE. If N_n^* reprasent the level population in LTE of a state characterized by quantum number n, and N_n represents its actual level population, then we define what is called the departure coefficient b_n by

$$N_n = b_n N_n^* \qquad (2.66)$$

When $b_n = 1$ for all bound levels, then LTE prevails. Even when $b_n = 1$ only for a subset of levels as a result of frequent collisions, then it is usual to refer to these states as being in LTE.

As discussed earlier, electron-electron, electron-ion and ion-ion collisions in an HII region, quickly thermalize the gas and all the particles will have a Maxweliian velocity

distribution characterized by a temperature T_e. But the population of quantum levels of interest for recombination lines, as the term itself suggests, is governed largely by recombination and one would therefore expect departures from a Boltzmann distribution ($b_n \neq 1$). However, for high principal quantum number states ($n > 100$ or so), the electron is loosely bound to the nucleus and collisions can induce transitions between levels thereby making the departure coefficients approach unity. This is further aided by the fact that the spontaneous transition probabilities go as n^{-5} which increases the radiative life times of large n levels thereby giving a chance for collisions to induce transitions between them On the other hand, the electrons in smaller n levels are more tightly bound to the nucleus and collisions will have a smaller influence on them In addition, their radiative life times are shorter. The population of the lower n levels are therefore determined largely by downward radiative transitions from higher n levels. One would therefore expect the departure from LTE to increase as n decreases.

The departure coefficients b_n decribe the actual population of a given level. The derivative of b_n with respect to n will decide the relative populations between adjacent levels. Therefore, the intensity of the recombination line will deviate from what is expected according to LTE depending on the magnitude and derivative of the departure coefficients

2.5. I The b_n calculation

The departure coefficients b_n are calculated using the criterion of time independant statistical equilibrium, which requires that there are as many transitions into a level as there are transitions out of it. The transitions to and from a level occur through several radiative and collisional processes. Some of the processes which are taken into account while setting up the equation for statistical equilibrium are

1. Spontaneous emission to lower levels

2. Cascade from higher levels

3. Radiative recombination

4. Induced emission and absorption between adjacent levels due to external radiation

5. Collisional transitions to adjacent levels

6. Collisional transitions to the continuum

7. Three body collisional recombination

8. Dielectronic recombination (in atoms with more than 1 electron)

The statistical equilibrium equation for all the levels is an infinite set of equations which should be solved simultaneously to obtain the b_n factors. To make the problem solvable it is necessary to assume that $b_n = 1$ for $n > n_{max}$ (usually $\sim$1000). This is a reasonable assumption to make since for these n collisions dominate and LTE is ensured. Usually, the equations are solved using what is known as case B in which it is assumed that the radiation due to recombination to the ground state is reabsorbed within the nebula and all the other radiation escapes freely. This assumption simplifies the calculation. The computations are further simplified for levels of interest in the radio region ($n > 40$) since the sublevels of different orbital angular momentum l are populated in accordance with their statistical weights. This results from collisions with protons which become more rapid for higher n, while the spontaneous downward radiative probabilities diminish markedly (αn^{-5}). The cross sections for different processes which populate and depopulate the level are taken from theoretical calculations.

One of the important factors that must be considered while calculating the departure coefficients, particularly for low density regions, is the external radition which can induce transitions between the levels, and affect the level populations. The external radiation can be due to an adjacent HII region, a

non-thermal source, or the galactic non-thermal background. The last two of these can be particularly important at low frequencies (higher n) where they are most intense. The magnitude of the effect of external radiation will depend on the geometry of the cloud and the source of radiation. Usually an appropriate dilution factor for the radiation should be calculated depending on the geometry. Due to this dependence on geometry it is not possible to have a unique set of theoretical b_n values for the different conditions of temperature and density found in nebulae. However, the effect of radiation becomes important only for very low densities ($< 0.1 cm^{-3}$) and for high quantum number levels ($n > 250$).

Considerable effort has gone into calculating the departure coefficietns b_n and their derivatives $(d b_n/dn)$ for a variety of conditions in HII regions and cold clouds (for eg. Sejnowski and Hjellming 1969, Brocklehurst 1970, 1971, 1973, Dupree 1972, Shaver 1975, Salem and Brocklehurst 1979). A computer program for calculating the departure coefficients has been published by Brocklehurst and Salem (1977). Many of the above references contain tables of b_n and it derivatives for a range of n values and different temperatures and densities.

Figure 2.7 show the b_n values as a function of quantum number n taken from calculations of Sejnowski and Hjellming (1969), for a typical electron temperature and different densities. The variation of b_n with n for different densities is as expected. For very large n the electrons are loosely bound to the nucleus and the radiative life times are long. Collisions dominate their population making them approach LTE. The b_n values therefore increase and approach unity as n increases. When n decreases collisions start losing their influence and radiative processes begin to take over making the departure from LTE much larger. As n is further decreased purely radiative processes influence the population and the b_n curves show an asymptotic behaviour.

As the density N_e increases, collisions become more frequent

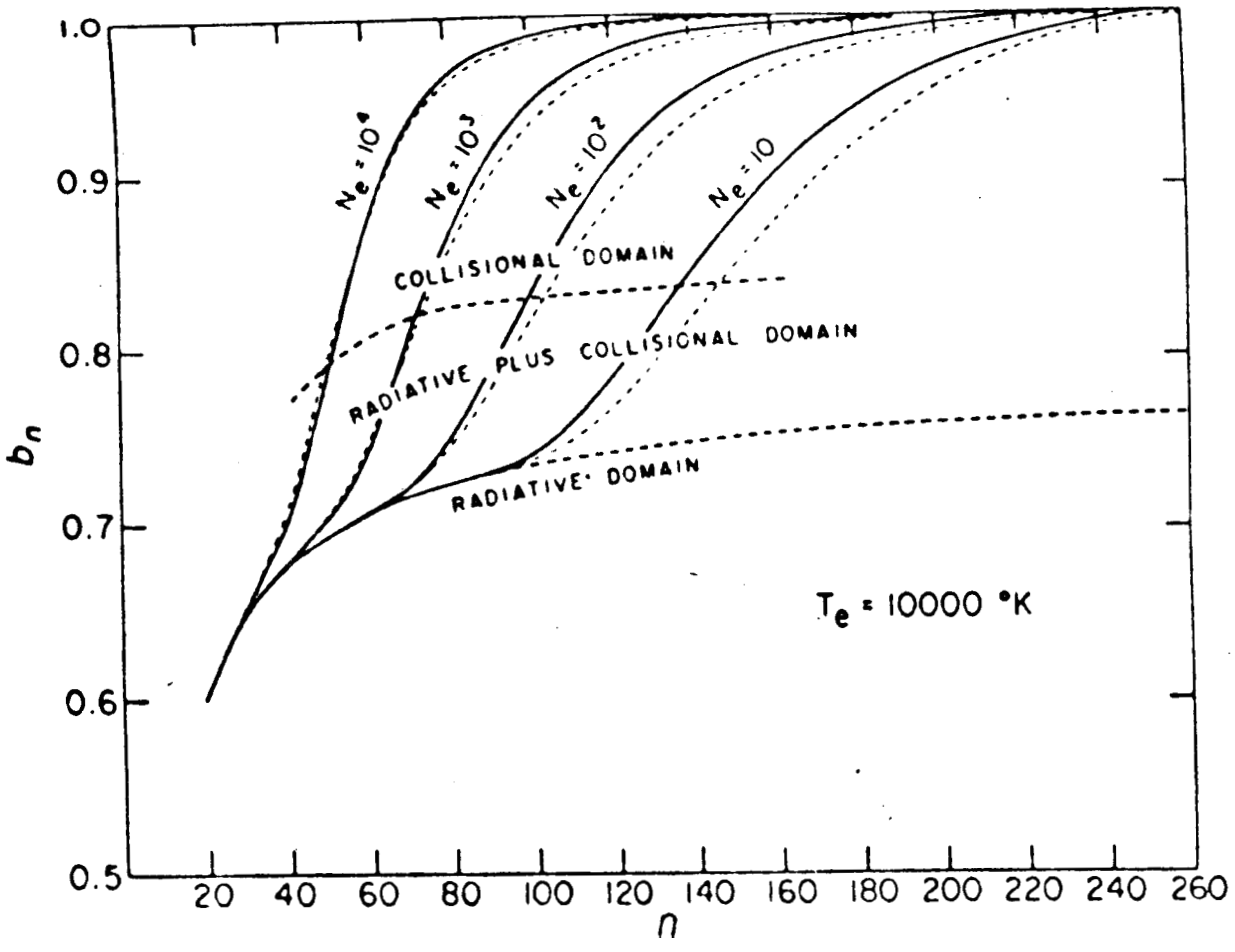

Fig. 2.7 The departure coefficients b_n as a function of principal quantum number n. (from calculation of Sejnowski and Hjellming 1969). The curves are shown for different electron densities N_e and a typical electron temperature.

thereby influencing lower n levels. The collisional domain then extends to lower n and the radiative domain is pushed further down. Therefore for a given n, as density increases the b_n factors increase and approach unity for very large densities.

2.5.2 Non-LTE Optical Depth

The non-LTE line absorption coefficient K_L is given by the net difference between absorption and emission between an upper level m and a lower level n

$$K_L = \frac{h\nu}{4\pi}\,\phi(\nu)\,(b_n N_n^* B_{nm} - b_m N_m^* B_{mn}) \qquad (2.67)$$

$$= \frac{h\nu}{4\pi}\,\phi(\nu)\,b_n N_n^* B_{nm}\left(1 - \frac{b_m}{b_n}\,\frac{N_m^* B_{mn}}{N_n^* B_{nm}}\right)$$

Using equations (2.40) to (2.42) we can write

$$K_L = b_n \beta_n K_L^* \qquad (2.68)$$

where

$$\beta_n = \left(1 - \frac{b_m}{b_n} e^{-h\nu/kT_e}\right) \Big/ \left(1 - e^{-h\nu/kT_e}\right) \qquad (2.69)$$

The quantity β_n is the ratio of the correction factor for stimulated emission in non-LTE to the corresponding factor in LTE (Goldberg 1966). Using the fact that in the radio region $h\nu/kT_e << 1$ we can write

$$\beta_n = \left(1 - \frac{\Delta b}{b_n} \cdot \frac{kT_e}{h\nu}\right)$$

where $\Delta b = b_m - b_n$. If $b >> \Delta b$ then $\frac{\Delta b}{b_n} \approx \frac{d \ln b_n}{dn}$ whence

$$\beta_n = \left(1 - \frac{kT_e}{h\nu}\,\frac{d \ln b_n}{dn}\right) \qquad (2.70)$$

The non-LTE optical depth is given by

$$\tau_L = \int_0^L K_L\,ds = b_n \beta_n \int_0^L K_L^*\,ds = b_n \beta_n \tau_L^* \qquad (2.71)$$

The line emission coefficient at a frequency ν is given by

$$j_L = N_m A_{mn} \frac{h\nu}{4\pi}\,\phi(\nu)$$

$$= b_m N_m^* A_{mn} \frac{h\nu}{4\pi}\,\phi(\nu) = b_m j_L^* \qquad (2.72)$$

where j_L^* is the LTE emission coefficeint.

2.5.3 Stimulated Emission

The quantity β_n in equation (2.69) is the ratio of stimulated emission in the non-LTE case to that in LTE. Since β_n appears as a direct multiplicative factor in the formula for the non-LTE optical depth (eqn 2.71), its sign and magnitude are crucial in deciding the line intensities. The value of β_n is given by the derivative of the departure coefficient b_n with respect to n (eqn 2.70) and therefore its magnitude and sign determines the relative populations of adjacent levels.

For most of the typical conditions in HII regions, and in cold clouds the value of β_n computed from the calculated values of b_n turns out to be negative over a certain range of frequencies depending on the density and temperature. A negative β_n results in a negative line optical depth (eqn 2.71). Since the line optical depth is directly proportional to the difference between the population of the upper and lower levels (eqn 2.67) a negative optical depth implies inversion of level poppulation and this causes stimulated emission to exceed absorption. It is easy to see that for the quantum levles of interest at radio frequencies, even slight departures from LTE can cause inversion of level populations. At radio frequencies $h\nu/kT_e \ll 1$ and therefore the ratio of level populations in LTE, which is proportional to $\exp(-h\nu/kT_e)$ is very close to unity. Therefore even small differences in the b_n values for adjacent levels (the derivative of b_n) can result in inversion of the population. The importance of this was first emphasized by Goldberg(1966).

Given an inverted population, stimulated emission of recombination lines can occur either due to the continuum radiation of the HII region itself or due to radiation from a background source. The importance of stimulated emission would depend on the magnitude of the β_n factors and the strength of the background continuum radiation. Calculations have shown (see for eg. Brocklehurst 1970, Shaver 1975, Salem and Brocklehurst 1979)

that the magnitudes of β_n are large at low frequencies (< 500MHz) for low density ionized regions. Fortuitously it is at these low frequencies that the non-thermal sources and the galactic background are most intense. As first pointed out by Shaver (1975) it is to be expected that low frequency recombination lines would be dominated by stimulated emission in low density regions.

We shall note here that although the line optical depth is negative and the populations are indeed inverted (except when $\beta_n > 0$), the stimulated emission of recombination lines is often referred to as 'partial masering'. This is perhaps because the total optical depth at the line frequency which is the sum of the continuum and line optical depth ($\tau_L + \tau_c$) may not be negative as in the case of OH or H_2O masers. However under some conditions (for example in partially ionized cold clouds), it is indeed possible to have $|\tau_L| > \tau_c$ at low frequencies, making the total optical depth negative. It would then result in a true maser.

2.5.4 Non-LTE Line Intensities

To compute the non-LTE line intensity we can use equation (2.33) and we will need the non-LTE source function given by

$$S_\nu = \frac{j_L + j_c}{k_L + k_c} = \frac{b_m j_L^* + j_c}{k_L + k_c}$$

The source function can be written in terms of the Planck function $B(T_e)$ using Kirchoff's law that

$$B(T_e) = \frac{j_L^*}{k_L^*} = \frac{j_c}{k_c}$$

The non-LTE source function is then given by

$$S_\nu = B(T_e)\,\frac{b_m k_L^* + k_c}{k_L + k_c}$$

which can also be written as $S_\nu = B(T_e)\,\dfrac{b_m \tau_L^* + \tau_c}{\tau_L + \tau_c}$ (2.73)

The intensity of the radiation received by an observer is given by equation (2.33) as

$$I_\nu = I_0 e^{-\tau_\nu} + S_\nu (1-e^{-\tau_\nu}) + \frac{I_N}{\tau_\nu}(1-e^{-\tau_\nu})$$

where $\tau_\nu = \tau_L + \tau_c$ is the total optical depth at a frequency ν. Using equations (2.73) and (2.5) we can rewrite the above equation for the total line and continuum temperature as

$$T_{L+C} = T_0 e^{-(\tau_L+\tau_c)} + \left(\frac{T_e(b_m \tau_L^* + \tau_c) + T_N}{\tau_L + \tau_c}\right)(1-e^{-(\tau_L+\tau_c)}) + T_F \quad (2.75)$$

where T_F is the foreground radiation. Outside the line frequency $\tau_L = 0$ and we have

$$T_c = T_0 e^{-\tau_c} + T_e(1-e^{-\tau_c}) + \frac{T_N}{\tau_c}(1-e^{-\tau_c}) + T_F \quad (2.76)$$

The excess temperature at the line frequency is the difference between equations (2.75) and (2.76)

$$T_L = T_{L+C} - T_c = T_0\left(e^{-\tau_c}(e^{-\tau_L}-1)\right) + T_e\left(\left(\frac{b_m \tau_L^* + \tau_c}{\tau_L+\tau_c}\right)(1-e^{-(\tau_L+\tau_c)}) - (1-e^{-\tau_c})\right) + T_N\left(\frac{1-e^{-\tau_L+\tau_c}}{\tau_L+\tau_c} - \frac{1-e^{-\tau_c}}{\tau_c}\right) \quad (2.77)$$

The first term in equation (2.77) is the contribution to the line temperature due to a source of brightness temperature T_o located behind the cloud. The second term is the instrinsic recombination line emission from the cloud itself and the last term is the contribution due to the non-thermal galactic background radiation distributed inside the cloud. Except when the pathlength through the could is very large (eg. a distributed medium), the contribution from the last term can be neglected.

Given T_o, T_e and T_N the above equation can be used to compute the expected recombination line temperature at any frequency. The line optical depth τ_L can be calculated for a given density and emission measure of the gas, using equations (2.71), (2.481, (2.57), (2.51) and (2.53). The continuum optical depth τ_c for the

same gas can be calculated using equation (2.13). The departure coefficeints b_n and their derivative β_n can be obtained from published tables (eg. Salem and Brockelhurst 1979) or calculated using the computer' program of Brocklehurst and Salem (1977). Appropriate beam dilution factors should be used if the different sources of radiation represented in equation (2.77) do not fill the beam of the telescope used for observations.

2.5.4.1 Isolated HII region: -

For an isolated HII region $T_o = 0$ in equation (2.77). Since the size of an HII region is at the most a few tens of parsecs, we can neglect the contribution due to the distributed non-thermal background i.e. $T_N = 0$.

In the optically thin case when $\tau_L^* \ll |\tau_L| \ll \tau_c \ll 1$ equation (2.77) reduces to

$$T_L = T_e \left(b_m \tau_L^* - \frac{\tau_L \tau_c}{2} \right) \qquad (2.78)$$

Using eqn (2.59) and (2.71) the ratio of LTE and non-LTE line intensities is given by

$$\frac{T_L}{T_L^*} = b_m \left(1 - \frac{\tau_c}{2} \beta_n \right) \qquad (2.79)$$

The quantity β_n (eqn 2.70) is usually negative for typical conditions found in HII regions. Therefore the line intensities are enhanced over the LTE expected value. The line enhancement in this case is due to stimulated emission in the presence of the continuum radiation of the HII region itself. From the calculated values of β_n it is seen that the enhancement increases at low frequencies. Consequently the electron temperature calculated from the measured line intensities using equation (2.63) are often underestimates.

In an optically thick case i.e. $\tau_c \gg 1.$, we can write

$$T_L = T_e \left[(b_m \tau_L^* + \tau_c) \left(\frac{1 - e^{-\tau_L + \tau_c}}{\tau_L + \tau_c} \right) - 1 \right] \qquad (2.80)$$

τ_L can be negative as β_n is usually negative. If we consider $|\tau_L| \approx \tau_c$ for example, then the region is transparent at the line frequency and we have

$$T_L = T_e [b_m \tau_L^* + \tau_c] \qquad (2.81)$$

Therefore even when the region is optically thick in the continuum it is possible to have strong emission recombination lines due to non-LTE effects, that is if β_n is negative and very large. If $|\tau_L| >> \tau_c$ and $\tau_L^* << \tau_c$ then

$$T_L = - T_e \left(\frac{\tau_c}{\tau_L} e^{-\tau_L} + 1 \right) \qquad (2.82)$$

As τ_L is negative the region again produces strong emission lines.

2.5.4.2 A cloud in front of a strong background source: -

If the cloud is not very large (< a few tens of parsecs along the line of sight) then the distributed non-thermal radiation T within.the cloud can be neglected in eqn (2.77)

In the optically thin case where $\tau_L^* << |\tau_L| << \tau_c << 1$ eqn (2.77) reduces to

$$T_L = T_e \left(b_m \tau_L^* - \frac{\tau_L \tau_c}{2} \right) - T_0 \tau_L \qquad (2.83)$$

Since τ_L is usually negative the last term in equation (2.83) results in stimulated emission of recombination lines in the presence of the background source with temperature T_o. For a non-thermal background source, T_o increases at low frequencies and the intensity of the recombination line can be dominated by stimulated emission. This will be so particularly for low density regions as they will be still optically thin at low frequencies and $|\beta_n|$ values are very large.

If β_n is positive, then the line optical depth τ_L is positive. If the temperature of the could is low (for example an HI cloud) then at low frequencies $T_o >> T_e$ and equation (2.83)

suggests the possibility of observing the recombination line in absorption. In fact such a line in absorption has been detected by Konevalenko and Sodin (1980, 1981) in the direction of the strong non-thermal source Cas A at 26 MHz and is attributed to carbon by Blake et al(1980).

In the optically thick case assuming τ_L to be negative and $|\tau_L| >> \tau_c >> \tau_L^* >> 1$ equation (2.77) becomes

$$T_L = T_0 e^{-\tau_L} - T_e \left(\frac{\tau_c}{\tau_L} e^{-\tau_L} + 1 \right)$$

Therefore an otherwise opaque cloud will feature prominent emission lines if $|\tau_L| >> \tau_c$. If $|\tau_L| \approx \tau_c$ then the region is transparent at the line frequency. A positive value of τ_L will give rise to an absorption feature.

2.6 THEORETICAL LINE INTENSITIES FROM MODEL PLASMA CLOUDS

It is instructive to look at the theoretical line intensities of hydrogen recombination lines at different frequencies for typical ionized regions found in interstellar space. The discussion in this section is based entirely on the calculations of Shaver (1975).

Shaver (1975) selected five model plasma clouds broadly representing HII regions, the cloud and the intercloud component of the interstellar medium The parameters of the model clouds are indicated in Table 2.1. The characteristics of the recombination lines were evaluated by Shaver (1975) for each of the models as follows. The ratio of the non-LTE line optical depth to the LTE optical depth was calculated using eqn (2.71) and b_n and β_n values for models A, B and C taken from Brocklehurst (1970). For models D and E Shaver (1975) separately calculated the b_ns incorporating the effect of the galactic non-thermal radiation field. The expected line temperature was calculated using equation (2.77) with $T_0 = T_N = 0$. The apparent amplification factor $e^{-\tau_c}(e^{-\tau_L} - 1)$ in equation (2.77) was also calculated for all models. In all the calculations the clouds

TABLE 2.1 : **Physical** parameters of model plasma clouds *

Model	T_e °K	N_e cm^{-3}	L PC	$\langle V_L^2 \rangle^{1/2}$ km/s	EM cm^{-6} pc
A	10000	I.0E+04	0.5	20	5.0E+07
B	5000	1.0E+2.5	5	20	5.0E+05
C	2500	10	50	20	5.0E+03
D	1000	0.05	10000	10	25
E	20	0.05	1000	10	2.5

* **Taken** from Shaver (I 975)

were assumed to fill the telescope beam at all frequencies.

Figure 2.8 shows the ratio of the non-LTE and LTE optical depths as a function of frequency for the different models. The ratio τ_L/τ_L^* gives the net induced emission over the LTE value. The peaks of these curves generally occur at frequencies an order of magnitude higher than those at which pressure broadening and optical depth effects become important. All these three factors contribute to the weakness of the lines at low frequencies. It is also clear from fig 2.8 that the optical depths are most affected by non-LTE effects when the density is low and the temperature is high, and at low frequencies.

Figure 2.9 shows the expected recombination line temperatures (with no beam dilution) for the different models as a function of frequency. The solid curves show the expected intensity in non-LTE, and the dashed ones in LTE calculated using eqn(2.77) with no background radiation ($T_b = T_N = 0$). Figure 2.9 shows that the strongest intrinsic recombination lines are those due to high density HII regions at frequencies between 1 and 10 GHz. At low frequencies the dominant lines are due to interstellar gas of lower densities. These lines are however not very intense.

The difficulty of detection of low frequency lines is somewhat reduced due to the masing charecteristics of these lines. Figure 2.10 shows the apparent amplification factor due to negative absorption at the line frequency for the different clouds. The line strength increases in proportion to the stength of the background source. Fortuitously it is just at these low frequencies that the discrete non-thermal sources and the galactic radiation field are the strongest. The amplification due to masing is particularly large for low density cold plasmas, and the line strength is only limited by the intensity of the background source. The dotted line in fig 2.8 represents the expected intensity for model E when a strong non-thermal source (T_b =100,000K at 100MHz and $\alpha = -2.6$) is located behind the cloud. From these curves it is clear that the most favourable

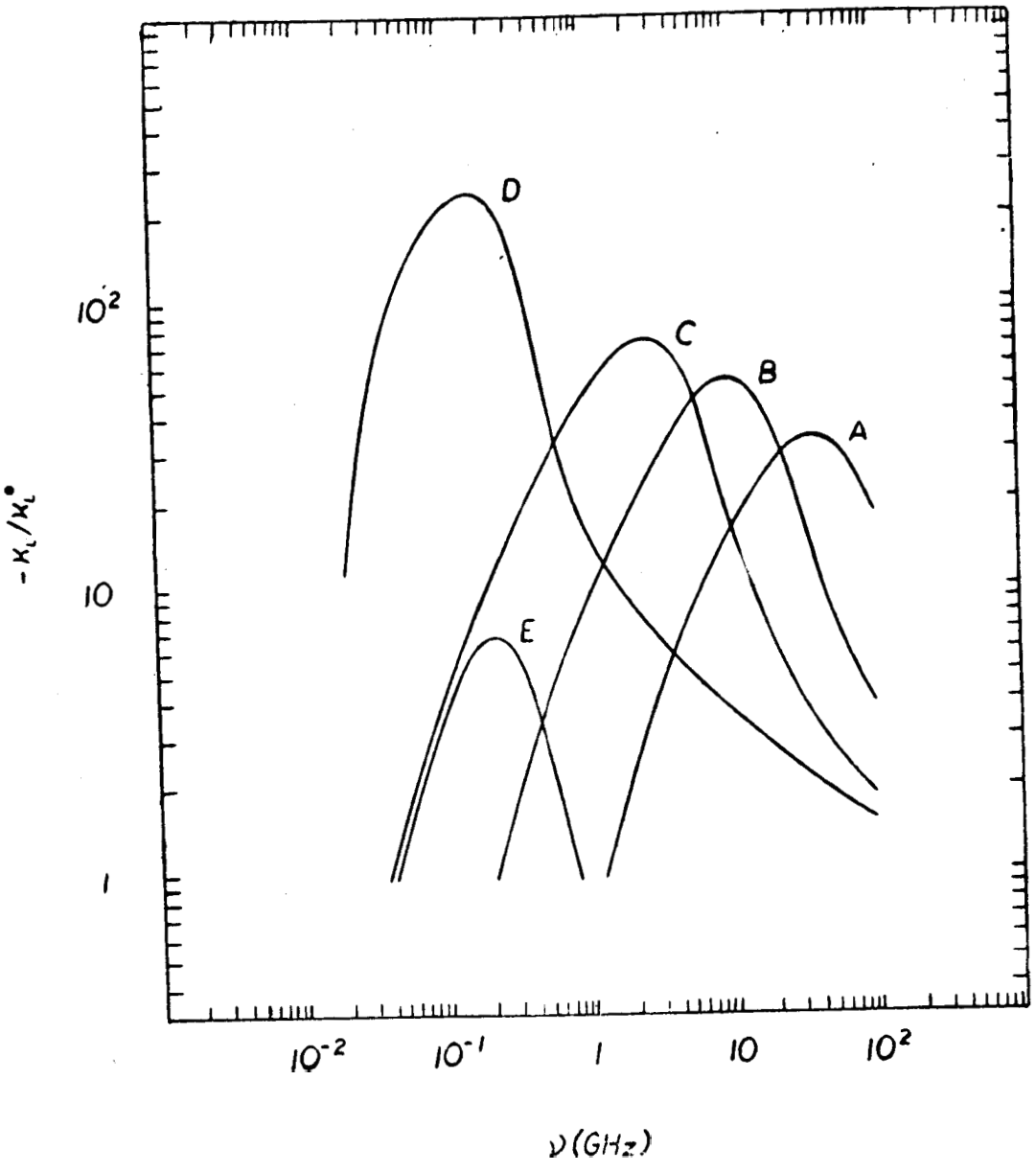

Fig. 2.8 The ratio of non–LTE and LTE absorption coefficients as a function of .frequency calculated by Shaver (1975) for the different model clouds (see tabel 2.1).

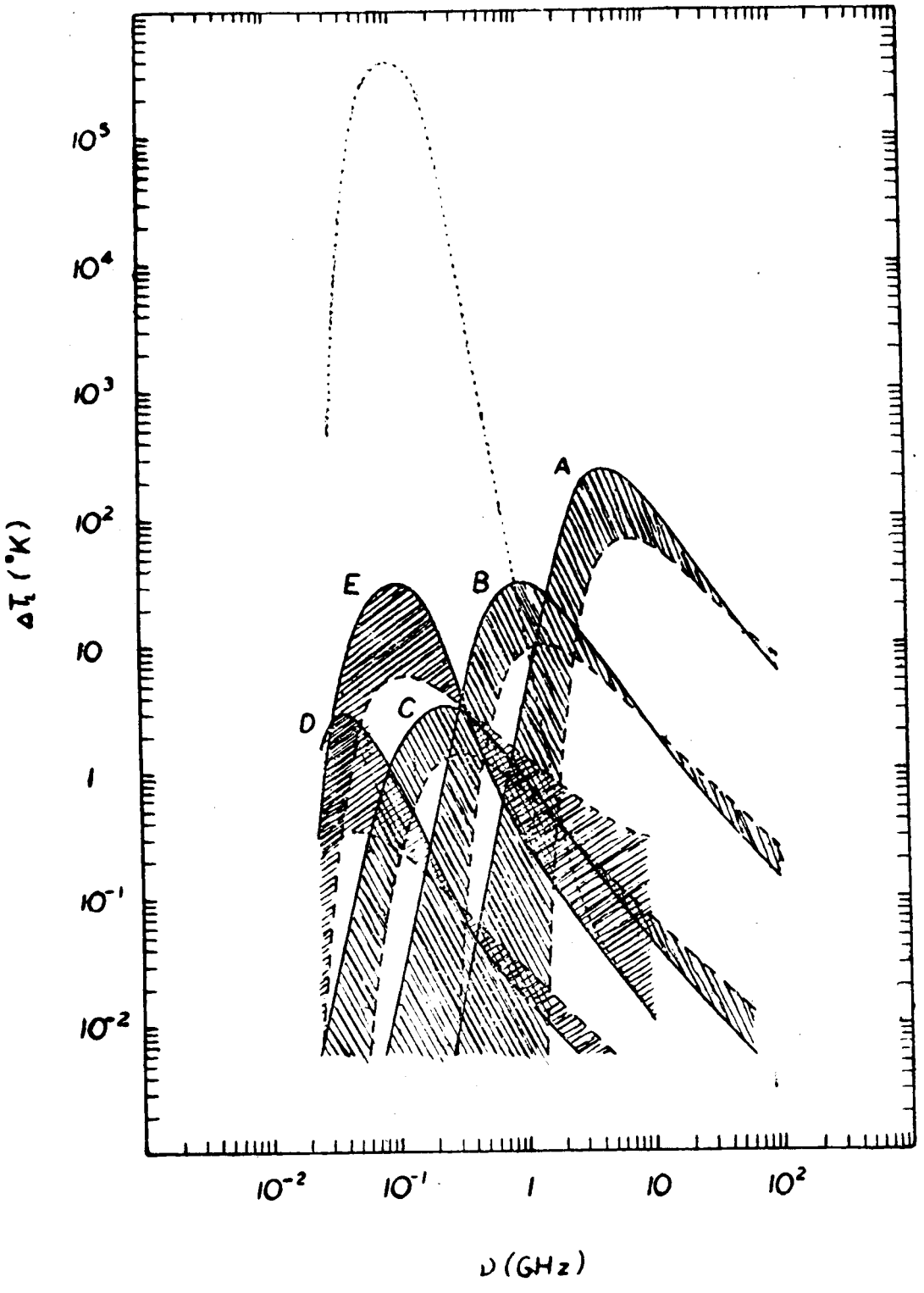

Fig. 2.9 Expected peak line temperature as a function of frequency for different models (see Table 2.1). The solid and dashed curves represent LTE and non–LTE conditions respectively. The dotted curve is the non–LTE case for model E when there is a strong non–thermal background source. (Taken from Shaver, 1975).

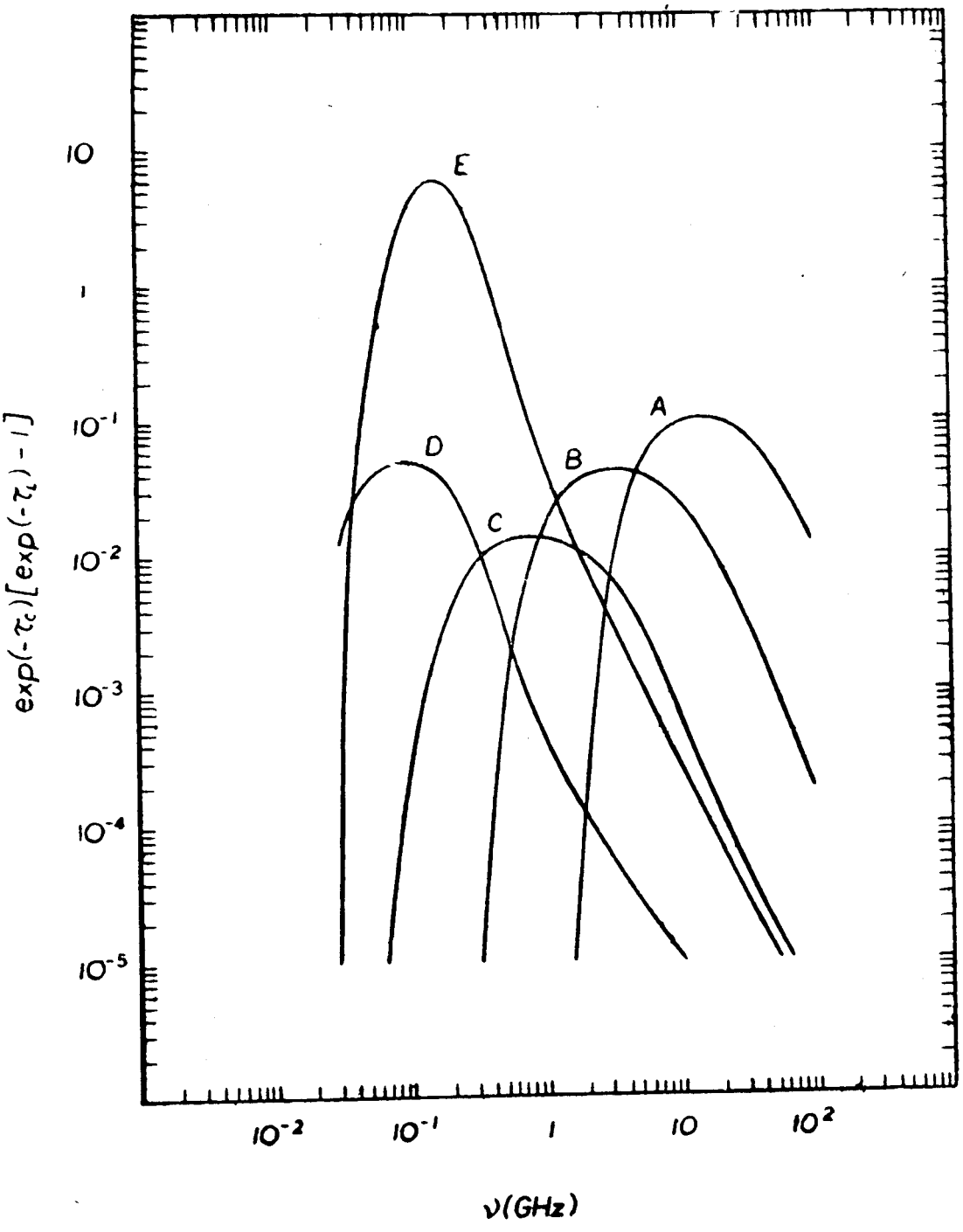

Fig. 2.10 Apparent amplification factor for the different model plasma clouds as a function of frequency (Taken from Shaver, 1975).

frequencies for observing masing lines from cold clouds are the intercloud medium are in the range of 100-200MHz which is somewhat below our observing frequency of 325MHz.

To summarize, at the low frequencies of interest to us (< 500MHz) the recombination lines will be dominated by low density ionized gas. The low continuum optical depth, the reduced effect of pressure broadening, the large amplification factors and the presence of intense background sources all contribute to its dominance at low frequencies. On the other hand, at these frequencies recombination lines from high density regions will be suppressed due to effects of optical depth, pressure broadening and low amplification factors. In addition, the poor angular resolutions available at low frequencies make the beam dilutions more severe for high density, small angular size regions whereas they are not so important for extended low density regions.